Prediction formula for the spectral wave period $T_{m-1,0}$ on mildly sloping shallow foreshores

Hofland, Bas; Chen, Xuexue; Altomare, Corrado; Oosterlo, Patrick

DOI
10.1016/j.coastaleng.2017.02.005

Publication date
2017

Document Version
Accepted author manuscript

Published in
Coastal Engineering

Citation (APA)
Hofland, B., Chen, X., Altomare, C., & Oosterlo, P. (2017). Prediction formula for the spectral wave period $T_{m-1,0}$ on mildly sloping shallow foreshores. *Coastal Engineering*, *123*(May), 21-28. https://doi.org/10.1016/j.coastaleng.2017.02.005

Important note
To cite this publication, please use the final published version (if applicable).
Please check the document version above.

Second Revision. Accepted for publication in Coastal Engineering.

Postprint of Coastal Engineering Volume 123, May 2017, Pages 21–28
Link to formal publication (Elsevier): https://dx.doi.org/10.1016/j.coastaleng.2017.02.005

Prediction formula for the spectral wave period $T_{m-1,0}$ on mildly sloping shallow foreshores

Bas Hofland
Delft University of Technology, Delft, The Netherlands, b.hofland@tudelft.nl
Deltares, Delft, The Netherlands
Xuexue Chen
Delft University of Technology, Delft, The Netherlands, X.Chen-2@tudelft.nl
Corrado Altomare
Flanders Hydraulics Laboratory, Antwerp, Belgium, corrado.altomare@mow.vlaanderen.be
Ghent University, Ghent, Belgium
Patrick Oosterlo
Delft University of Technology, Delft, The Netherlands, P.Oosterlo@tudelft.nl

Abstract

During the last decades, the spectral wave period $T_{m-1,0}$ has become accepted as a characteristic wave period when describing the hydraulic attack on coastal structures, especially over shallow foreshores. In this study, we derive an empirical prediction formula for $T_{m-1,0}$ on shallow to extremely shallow foreshores with a mild slope. The formula was determined based on flume tests and numerical calculations, mainly for straight linear foreshore slopes. It is shown that the wave period increases drastically when the water depth decreases; up to eight times the offshore value. The bed slope angle influences the wave period slightly. For short-crested wave fields, the strong increase of $T_{m-1,0}$ starts closer to shore (at smaller water depths) than for long-crested wave fields.

Keywords

spectral wave period, $T_{m-1,0}$, shallow foreshore, very shallow foreshore, sea dike, infragravity waves

1. Introduction

During the last decades, the spectral wave period $T_{m-1,0}$ has been accepted as a characteristic period when describing the interaction between sea waves and coastal structures. This wave period is used for describing many processes like wave run-up, overtopping, reflection, and armour layer stability, especially when the structure has a shallow foreshore. The period can

also be used in situations characterized by a multi-modal wave spectrum. It is sometimes called the wave energy period as it is the equivalent wave period needed to calculate the energy flux P for any irregular wave field in deep water: $P \propto {H_{\mathrm{m0}}}^2 T_{m-1,0}$ (e.g. Battjes, 1969), where H_{m0} is the spectral significant wave height.

In the present study, a foreshore is defined as the part of the seabed bathymetry seaward of the toe of a structure that has influence on waves. The configuration considered in this paper is shown in Figure 1. A shallow foreshore is typically characterized by depths smaller than about three to four times the significant wave height. A very shallow foreshore may be further defined where the wave height is reduced to about 50% of its offshore value. Such foreshores are considered to be mildly sloping when the slopes are gentler than 1:30, such that the waves are influenced by depth-effects over a certain distance. These definitions are discussed in more detail in Section 2.2.

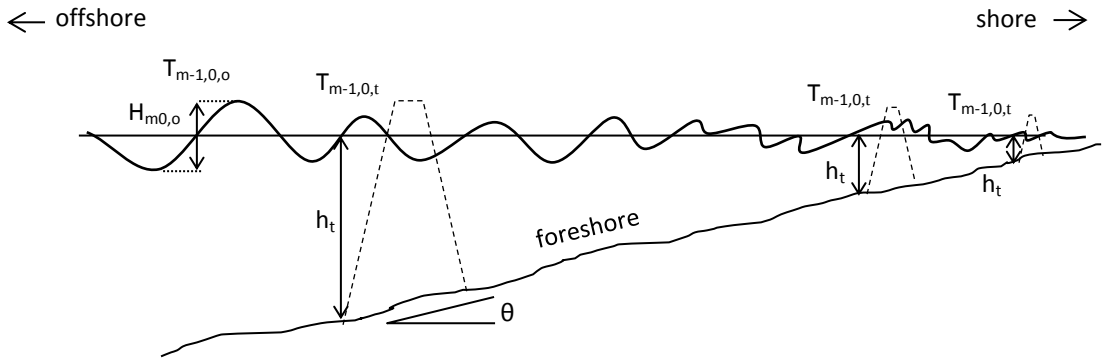

Figure 1. The foreshore configuration that is treated in this study. Three possible locations for structures on the sea bed are indicated, as well as the conditions at the toes of these structures, $T_{m-1,0,t}$ and h_t. The offshore conditions are indicated by the offshore spectral wave period $T_{m-1,0,o}$ and the offshore wave height $H_{m0,o}$.

Hard-soft hybrid constructions, for example dike-in-dune constructions or large beach nourishments in front of sea walls such as those found in the Netherlands and Belgium, are characterized by large amounts of sand seaward of the hard structure. Therefore, once the sand has been eroded away in an extreme storm, the foreshore in front of the hard dike will be extremely shallow (in the order of one metre). In these situations, the magnitude of the wave period is not well known, although very large wave periods have been observed on shallow foreshores. Usually numerical or physical modelling is applied to predict the wave period, or the response of the structures directly (Van Gent, 1999a,b; Van Gent, 2004; Suzuki et al., 2014; Altomare et al., 2016). Design formulas for several types of response in these conditions do exist, however the near shore wave period is often required in these equations.

While the significant wave height H_{m0} at the local depth h over a shallow foreshore can be predicted relatively well using a value for the breaker parameter H_{m0}/h (e.g. Goda,1975, CIRIA et al., 2007), to the authors' knowledge no empirical formula exists for the prediction of the wave period $T_{m-1,0,t}$. Therefore, an empirical formula to predict the wave period is proposed, which is calibrated using various data sets that have been gathered in shallow and very shallow foreshores in the Netherlands and Belgium.

In this paper, first the existing knowledge on $T_{m-1,0}$ is treated in Section 2.1. Next, in Section 2.2, a classification of different types of shallow foreshore (shallow, very shallow, and extremely shallow) is presented, which is important for understanding the generation mechanism of low-frequency energy on such foreshores. In Section 2.3, relevant research about low-frequency waves is introduced. In Section 3 the datasets and the numerical calculations that are used to derive an empirical prediction formula for $T_{m-1,0}$ are described. Subsequently, the derived prediction formula is presented in Section 4. This paper ends with a discussion and conclusions in Sections 5 and 6.

2. Literature review

2.1 Spectral wave period, $T_{m-1,0}$

Many wave periods, such as the peak period T_p (defined as the frequency at the peak of the wave spectrum), and the significant zero-crossing period $T_{1/3}$ (mean period of the highest third of the waves) have been proven to be linked to many coastal processes for standard spectral shapes and deep water conditions. However, for shallow foreshores, the spectral shape tends to become flattened and/or double-peaked. Examples of wave spectrum shapes along different locations on shallow foreshores are presented in Figure 2. Spectral shapes like the ones presented in Figure 2 make most of these commonly used wave periods in deep water less suitable to describe the coastal processes in shallow water. To weigh the contribution of different parts of the spectrum to the relevant coastal process, several spectral periods are applied, for example $T_{m0,1}$ or $T_{m-1,0}$. The spectral period $T_{m-1,0}$ is defined as:

$$T_{m-1,0} = \frac{m_{-1}}{m_0} \quad , \text{ with } m_n = \int_0^\infty S\, f^n df \quad , \tag{1}$$

where f is frequency and S the spectral density of the water surface elevation. m_0 is the variance of the water surface elevation. The mean energy wave period, $T_{m-1,0}$, gives more

weight to the lower frequencies, and therefore to the longer periods in the spectrum, than wave periods like T_p or $T_{1/3}$.

After Holterman (1998) made the first attempt to link wave run-up to several wave periods based on moments of the wave spectrum, the period $T_{m-1,0,t}$ was recommended by Van Gent (1999a, 2001) as the best suited wave period to describe wave run-up and overtopping process for single and double-peaked spectra. Various spectral-based wave periods have been correlated to wave run-up and $T_{m-1,0,t}$ has been found to have the highest correlation. Therefore, the overtopping discharge can be computed for a given $T_{m-1,0,t}$ and wave height, independent of the type of spectrum. Subsequent research discovered and validated the correlation of $T_{m-1,0,t}$ to a number of coastal processes, e.g., wave overtopping (Van Gent, 1999a,b; Pozueta et al., 2005; Altomare et al., 2016), reflection (Dekker et al., 2007; Zanuttigh & Van der Meer, 2008), armour layer stability (Van Gent, 2004), and wave impacts (Chen et al., 2016). The use of $T_{m-1,0,t}$ is also incorporated in manuals such as the EurOtop manual (EurOtop, 2016) and the Rock Manual (CIRIA et al., 2007).

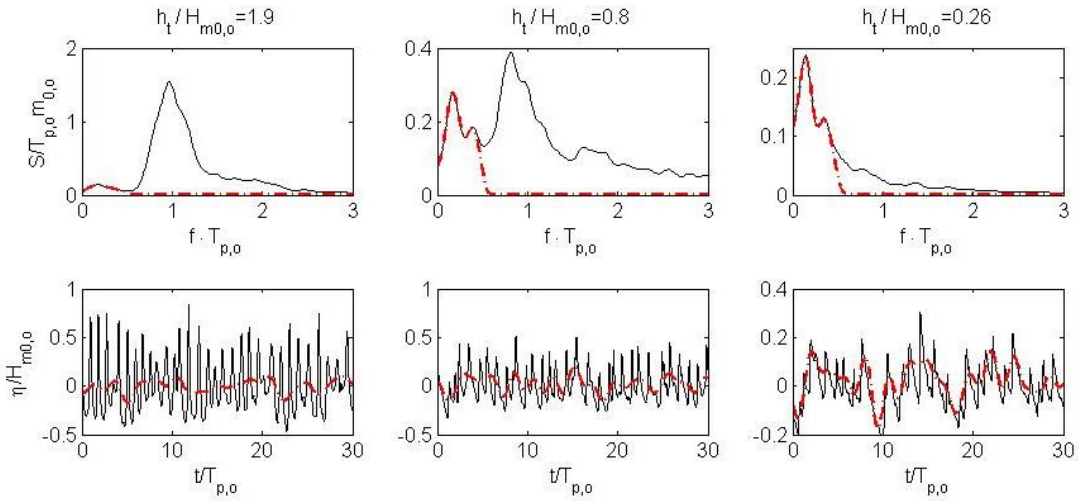

Figure 2. Example of measured wave spectra (top) and surface elevations η (bottom) for various water depths on a shallow foreshore, normalized by offshore wave parameters (subscript *o*) (data of Chen et al., 2016). The water depths are roughly indicated in Figure 1. Solid lines indicate the signals within the full frequency range, whereas the dash-dotted lines indicate the corresponding low-pass filtered signals (cut-off at $f_p/2$).

Presently, in engineering, the deep water ratio $T_{m-1,0,o} / T_{p,o} \approx 0.9$ for a single-peaked spectrum is often used to predict the wave period near the toe of a structure $T_{m-1,0,t}$ from a known offshore wave period $T_{p,o}$. Here the subscripts o and t represent the *offshore* and *toe* locations, respectively. Hence it is essentially stated that $T_{m-1,0,t} / T_{m-1,0,o} = 1$, independent of the location of the structure. The ratio of $T_{m-1,0,t} / T_{m-1,0,o}$ can actually reach values up to 8, as will be shown in Section 4. Therefore, the use of the ratio $T_{m-1,0,o} / T_{p,o}$ for the estimation of $T_{m-1,0,t}$ at

shallow foreshores is invalidated in this study. A prediction formula for $T_{m-1,0,t}$ over (very) shallow foreshores is thus required.

2.2 Foreshore

Goda (2009) argued that there is no agreement about the terminology of the word foreshore in many references. Manuals such as the Rock Manual (CIRIA et al., 2007) and Coastal Engineering Manual (USACE, 2002) formally define a foreshore as the part of a beach between a high and a low water level. However, in coastal structure research, the word foreshore is defined differently. It implies the part of the seabed bathymetry seaward of the toe of the structure that is characterized by depth-induced wave processes such as depth-induced wave breaking. In the EurOtop manual (EurOtop, 2016), for example, the foreshore is defined as the section in front of the dike/structure and it "can be horizontal or up to a maximum slope of 1:10 […] having a minimum length of one [fictitious deep water] wavelength L_o".

Because of wave breaking on a shallow foreshore, the wave height becomes depth limited. Moreover, there is not one clear peak frequency visible anymore in the energy density spectrum (e.g. Holterman, 1998, Van Gent, 2001). Also, using the Rayleigh distribution to calculate the distribution of wave heights and wave run-up levels in deep water cannot be applied anymore for shallow foreshores (e.g. Battjes and Groenendijk, 2000).

As certain formulae for e.g. wave overtopping or wave impact forces are intended to be used for shallow or very shallow foreshores, because their validity depends on the type of wave motion, it is required to characterize the shallowness of the foreshore explicitly. The shallowness of the foreshores is best characterized by the water depth near the structure, h_t, normalized by the offshore wave height $H_{m0,o}$. In literature, some (approximate) limits can be found with some interpretation for four classes of foreshore: deep, shallow, very shallow and extremely shallow, see Table 1. The prediction formula for $T_{m-1,0,t}$ presented in this paper includes all these classes of foreshores. The definitions of hydraulic and foreshore geometry parameters are illustrated in Figure 1.

Offshore is defined here as $h_t/H_{m0,o} > 4$, as that is the water depth at which no depth-induced wave breaking occurs according to the Battjes and Groenendijk (2000) equation. Other references (Holterman, 1998; TAW, 2002) give a similar limit of 3 to 4.

Shallow is defined here as $1 < h_t/H_{m0,o} < 4$. This is the depth where the water depth starts to influence the wave breaking. The wave spectrum observed here is still similar to that offshore

(here JONSWAP) with a clear single peak, but some minor (higher and lower) second-order effects are visible, see the left panels of Figure 2 where the typical wave signal on a shallow foreshore is depicted.

Very shallow is defined as $0.3 < h_t/H_{m0,o} < 1$. This is the water depth where the wave height is reduced to 50% to 60% of the offshore wave height by depth-induced wave breaking as defined by e.g. Holterman (1998), TAW (2002), and EurOtop (2016). As the breaker parameter ($H_{m0,t}/h_t$) on a mildly sloping foreshore is also somewhere between 0.5 to 0.6, that gives a definition of the shallow foreshore of $h_t/H_{m0,o} < 1$. Van Gent (1999a) presented data in the very shallow range, where the flattening of the spectra becomes apparent. In the middle panels of Figure 2 the typical wave signal on a very shallow foreshore is depicted. The majority of the offshore spectrum has been dissipated, and a large amount of low-frequency energy has emerged.

Extremely shallow is defined in the present paper as $h_t/H_{m0,o} < 0.3$, or more shallow than studied by Van Gent (1999a). In the right panels of Figure 2 the typical wave signal on an extremely shallow foreshore is depicted. Nearly most of the high frequency part of the spectrum has been dissipated, and the low-frequency energy is dominant. Altomare et al. (2016) and Chen et al. (2016) present data in this range.

Deep (Holterman, 1998; Battjes & Groenendijk, 2000; TAW, 2002)	$\frac{h_t}{H_{m0,o}} > 4$
Shallow (Holterman, 1998; TAW, 2002)	$1 < \frac{h_t}{H_{m0,o}} < 4$
Very Shallow (Van Gent, 1999)	$0.3 < \frac{h_t}{H_{m0,o}} < 1$
Extremely Shallow (Altomare et al., 2016; Chen et al., 2016)*	$\frac{h_t}{H_{m0,o}} < 0.3$

Table 1. Consistent classification of foreshore depths, based on the water depth at toe of structure h_t, normalized by the offshore wave height $H_{m0,o}$.
*) here different classifications are used.

Also other parameters are used to classify the shallowness of a foreshore, such as the steepness of the wave field (Altomare et al., 2016; EurOtop, 2016), or the surf-similarity parameter ξ (EurOtop, 2016). However, using these parameters, that include the local wave period, to classify foreshores is not convenient in the present research, as the aim is to obtain

a prediction of this local wave period. Moreover, non-breaking swells on deep foreshores would then formally also classify deeper foreshores as shallow foreshore, whereas shallow foreshore in the present context implies the presence of heavy wave breaking. When the surf-similarity parameter based on the structure slope is used to define a shallow foreshore, steep structure slopes would imply the presence of a shallow foreshore. This has no physical relevance.

2.3 Infragravity wave research

Munk (1949) and Tucker (1950) were the first to relate the presence of low-frequency or infragravity waves in the shoaling and surf zones to the group structure of the incident short waves. Infragravity waves are long waves of periods typically with an order of 100 s in prototype (Van Dongeren et al, 2007). Two generation mechanisms of this kind of waves have been identified: the shoaling of the low-frequency long waves, and the time-varying breakpoint mechanism (or surf-beat). Both these mechanisms are associated with the modulation of the wave height on the scale of the wave group. In the first mechanism, the variation in radiation stress at the time scale of the incident wave group forces bound infragravity waves (Longuet-Higgins and Stewart, 1962). These bound waves are in anti-phase with the forcing wave groups. Alternatively, the time varying location of the breakpoint, due to the group structure of the incident short waves, results in the generation of free low-frequency waves (Symonds et al., 1982). The type of generation mechanism seems to be dependent on the slope of the foreshore and steepness of the incoming (low-frequency) waves (Battjes et al., 2004, Van Dongeren et al., 2007). The first mechanism (shoaling of bound long waves) is believed to be dominant on a mild slope, where the mild slope is characterized by a low value of surf-similarity-like parameter, β_b:

$$\beta_b = \frac{\theta}{\omega}\sqrt{\frac{g}{h_b}}\,, \tag{2}$$

where θ is the bed slope, ω is the angular frequency of the long waves, h_b is the mean breaker depth of the primary short waves, and g the gravitational acceleration. In the mild slope regime ($\beta_b < 0.3$), the low-frequency waves are shown to be breaking, yielding a low reflection of the long waves (Van Gent, 2001; Van Dongeren et al., 2007).

The generation mechanisms of the low-frequency wave energy may be different for short-crested waves. Short-crested waves exhibit less long-wave energy generation on beaches (e.g.

Herbers et al., 1994) and less wave overtopping occurs at structures with very shallow foreshores when short-crested seas are applied (Suzuki et al., 2014).

In conclusion, there is much research on the origin on the low-frequency energy on (very) shallow foreshores. For the mildly sloping foreshores treated here, the generation of low-frequency energy appears to have a different generation mechanism than that for steep beaches. Moreover, the value of the wave period $T_{m-1,0}$ is influenced by the presence of low-frequency waves. This wave period is shown to be important for many wave-structure interaction processes, and can be used to assess the response of coastal structures with shallow foreshores. However, no empirical prediction tool is available to predict this wave period. This paper aims to provide such an engineering tool.

3. Data sets

In order to derive a prediction formula for $T_{m-1,0,t}$, several data sets of physical model studies have been selected, and some additional numerical calculations have been performed. An overview is given in Table 2. In the first part of this section the general set-up for all these studies is described, followed by the specifics of the separate studies.

In all studies, the bottom was horizontal from the wave maker to the toe of the foreshore, representing deep water (deeper than $4H_{m0,o}$). For all tests (except Deltares, 2011; and FHR13_168), the foreshore was characterized by an initial linear slope followed by a horizontal part, as shown in Figure 3. Furthermore, instead of having the sea dike, a horizontal platform was inserted just after the foreshore. Damping material (e.g. gravel or foam) was located after the platform to reduce the possible reflection of (long) waves as much as possible.

The waves (offshore and at the structure) were measured at the horizontal sections. Classical reflection analysis methods (e.g. Mansard and Funke, 1980) are not suitable in shallow water conditions because non-linear effects dominate in cases with very shallow foreshores (Van Gent, 1999a) and the presence of long waves. Instead, the measurements of wave height and period at the dike toe (h_t) have been conducted using a single wave gauge at the location of the (virtual) dike toe without the presence of the reflecting structure.

The wave conditions for all test series consisted of irregular waves with values for the offshore wave steepness, $s_{m-1,0,o} = H_{m0,o} / \frac{g}{2\pi} T_{m-1,0,o}^2$, ranging from around 0.01 to around 0.05. Typically standard JONSWAP spectra were applied.

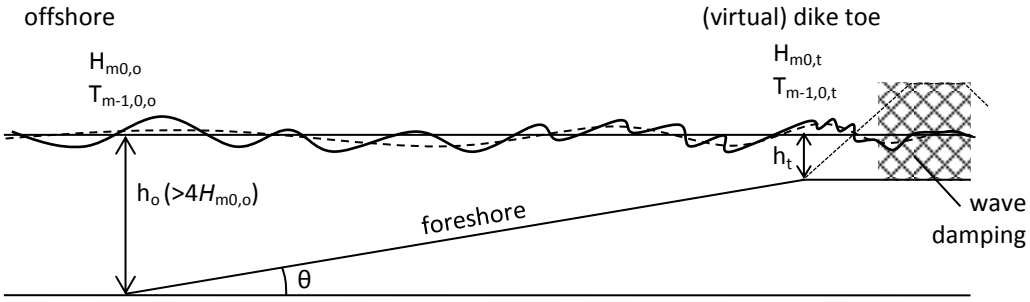

Figure 3. Typical setup for the model studies used. The dashed line indicates the (bound) long wave. h_o indicates the offshore water depth, and θ indicates the foreshore slope.

Van Gent (1999a) measured the wave parameters for foreshore slopes of 1:100 and 1:250 in the Scheldt Flume of Deltares (1 m × 1.2 m × 55 m). JONSWAP and double-peaked spectra were applied. The entire (smoothed) measured spectral range was utilized to determine the values of $T_{m-1,0,t}$. The waves were generated with Active Reflection Compensation and 2nd order wave generation.

Chen et al. (2016) measured the wave conditions in a wide flume (4 m × 1.4 m × 70 m) at Flanders Hydraulics Research (FHR). The foreshore extended over the entire width and was split in four sections around the top horizontal part. Passive wave absorption was present in the outer two sections, and at the two sections in the middle of the flume a dike section was present. The possible build-up of low (or high) frequency energy was investigated using wavelet analysis, and was absent. Only the energy corresponding to the first seiching mode was slightly increased. Hence, the entire spectrum was used to determine $T_{m-1,0,t}$, except for the frequency band corresponding to a slight seiching oscillation (over the small frequency resolution $\Delta f = 0.01$ Hz) that was removed. First order wave generation was used.

Altomare et al. (2016) describe three more experimental campaigns that have been carried out in the same wide flume at FHR between 2012 and 2015 (datasets: 13-116, 00-025, 13-168), having as main objectives the characterization of wave overtopping and loading on coastal defences with shallow to extremely shallow foreshores. The foreshore slopes were smooth. Passive reflection compensation, wave generation, and data processing were done in a similar fashion as Chen et al. (2016). For tests 13-168 the setup differed somewhat. It was characterized by a 1:50 (upper) foreshore slope with a length of 21 m. A 1:15 transition slope of 5 m long was constructed between the wave maker and the start of the foreshore to obtain a

sufficient depth at the wave maker location. Offshore wave heights of 2.4 to 7 cm were applied. In test series 13-168, 2nd order wave generation was used.

XBeach. The numerical model XBeach was used to model a similar setup as applied in the tests. XBeach is a nearshore numerical model used to assess the coastal response during storm conditions, and has extensively been calibrated and validated (Roelvink et al., 2009; Smit et al., 2010; www.xbeach.org). In the currently applied non-hydrostatic mode it solves the non-linear shallow water equations, including a non-hydrostatic pressure correction, based on the approach of Stelling and Zijlema (2003). The wave breaking behaviour is improved by disabling this non-hydrostatic pressure term when the water level gradient exceeds a certain steepness. After this, the bore-like dissipation term in the momentum-conserving shallow water equations takes over (Smit et al., 2010).

XBeach calculations were performed for the cases of Van Gent (1999a) with a JONSWAP spectrum, a 1:100 slope, and wave steepness $s_{m\text{-}1,0,o}$ = 0.043, as well as for additional shallower cases that were not tested. For these tests the value of $k_p h_o$ ranged from 0.63 to 1.18, where k_p is the wave number based on the peak period. The short wave celerity of wave components with $kh < 3$ is within 3%. The calculations are well below this limit, and with decreasing water depth the accuracy increases. To get well-converged statistics of the long bound waves, 5000 waves were used in the calculations. Furthermore, both long-crested (1D calculations) and short-crested (2D calculations) waves were used for all conditions. For the short-crested waves, a directional spreading with a standard deviation of $\sigma = 25°$ was applied. The main wave angle was normal to the coast line. The numerical flume was 45 m long (513 grid cells) for the 1D cases. The 2D calculations used the same length and a width of 40 m and 101 grid cells. For the bed friction, a friction coefficient of $c_f = 0.002$ (concrete bed) was used. At both the generation and the downstream side of the domain a weakly reflective boundary condition was used. For the 2D cases, periodic boundary conditions were applied at the lateral boundaries, to prevent edge effects. In the post-processing, the entire (smoothed) spectral range was used to determine the value of $T_{m\text{-}1,0}$.

Deltares (2011) obtained measurements of $T_{m\text{-}1,0,t}$ in a commercial project where an irregular natural shallow foreshore was applied. The foreshore slope was 1:10 up to h / $H_{m0,o} \approx 2.7$, followed by a horizontal part of about 3 m, and an irregular sloping part with a mean slope of about 1:200 to the toe of a 1:1.5 rubble mound slope. The foreshore was not constant over the width, and waves were travelling onto the slope under a 30° obliquity. Two test conditions were repeated with long- and short-crested waves, while all other conditions were identical.

Source	slope 1:cotθ	spectrum	lab.	h_t / $H_{m0,o}$	dir. spreading	# tests	order of wave generation
Van Gent, 1999	1:100	JONSWAP	Deltares	0.34-2.52	no	12	2nd
Van Gent, 1999	1:250	JONSWAP	Deltares	0.34-2.52	no	12	2nd
Van Gent, 1999	1:100	Double peaked	Deltares	0.67-2.52	no	30	2nd
Van Gent, 1999	1:250	Double peaked	Deltares	0.67-2.52	no	12	2nd
Chen et al., 2016	1:35	JONSWAP	Flanders Hydraulics	0.15-0.83	no	49	1st
Altomare et al., 2016 FHR13_116	1:35	JONSWAP	Flanders Hydraulics	-0.05-0.20	no	45	1st
Altomare et al., 2016 FHR00_025	1:35	JONSWAP	Flanders Hydraulics	-0.14-0.25	no	21	1st
XBeach calculations	1:100	JONSWAP	numerical, XBeach	0.08-2.52	no	9	2nd
XBeach calculations	1:100	JONSWAP	numerical, XBeach	0.08-2.52	σ=25°	9	2nd
Altomare et al., 2016 FHR13_168	1:15, 1:50	JONSWAP	Flanders Hydraulics	0.00-0.86	no	28	2nd
Deltares, 2011 (in-house data)	irreg.	JONSWAP	Deltares	1.34-1.37	σ=5°	2	1st
Deltares, 2011 (in-house data)	irreg.	JONSWAP	Deltares	1.34-1.37	σ=22°	2	1st

Table 2. Data sets used in this study.

4. Results

The data of Van Gent (1999a) and Chen et al. (2016) are plotted in the left graph of Figure 4, with the relative depth on the horizontal axis and the ratio of nearshore to offshore spectral wave period on the vertical axis. These data sets represent tests with a wide range in foreshore slopes over a comparable range of dimensionless depths. It can be seen that the wave periods increase with decreasing relative depth h_t/H_{m0} on the foreshore, but much scatter is present.

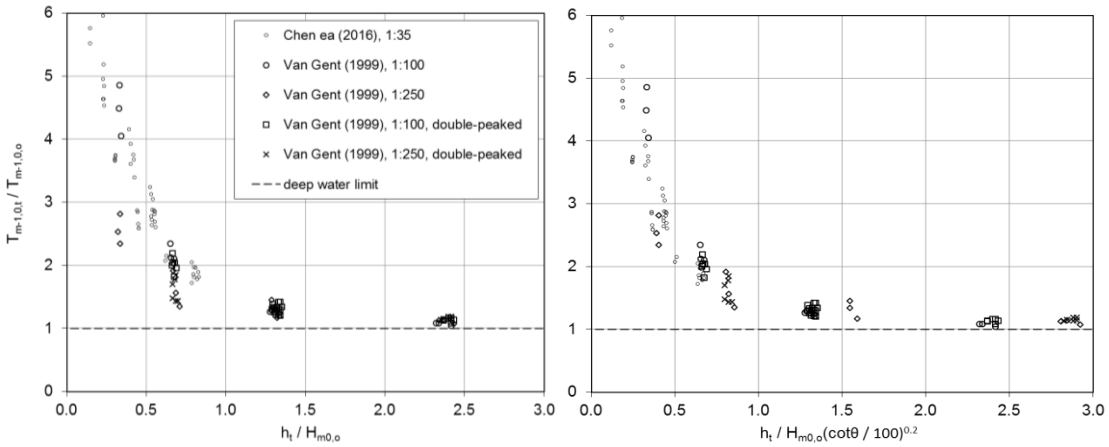

Figure 4. Measured evolution of wave period $T_{\text{m-1,0,t}}$ as function of relative water depth for selected flume tests with (right) and without (left) slope correction.

Next, a parameter is introduced in which, besides the relative depth, also the foreshore slope θ is incorporated as follows:

$$\tilde{h} = \frac{h_{\text{t}}}{H_{\text{m0,o}}}\left(\frac{\cot\theta}{100}\right)^{0.2} \quad . \tag{3}$$

Here θ is the slope angle of the foreshore. The exponent on the slope term is determined empirically, by minimizing the scatter. The inclusion of the slope seems to yield a slightly better data collapse, as shown in the right graph of Figure 4. The R^2-value (coefficient of determination) of the best fit (with a shape as presented later) was respectively 0.91 and 0.94 for these data, without and with the slope influence in the dimensionless foreshore depth formulation in eq. (3). Since the slope has an effect on the wave transformation processes according to eq. (2), this influence is credible. So, despite the limited improvement of the fit using this influence, it is maintained. According to eq. (2), a kind of surf-similarity parameter based on the foreshore slope like $\tan\theta/\sqrt{s_{\text{m-1,0,o}}}$ could be expected to be better related to the evolution of the low-frequency energy, and hence to the spectral wave period. However, the data collapse only deteriorated when using this parameter.

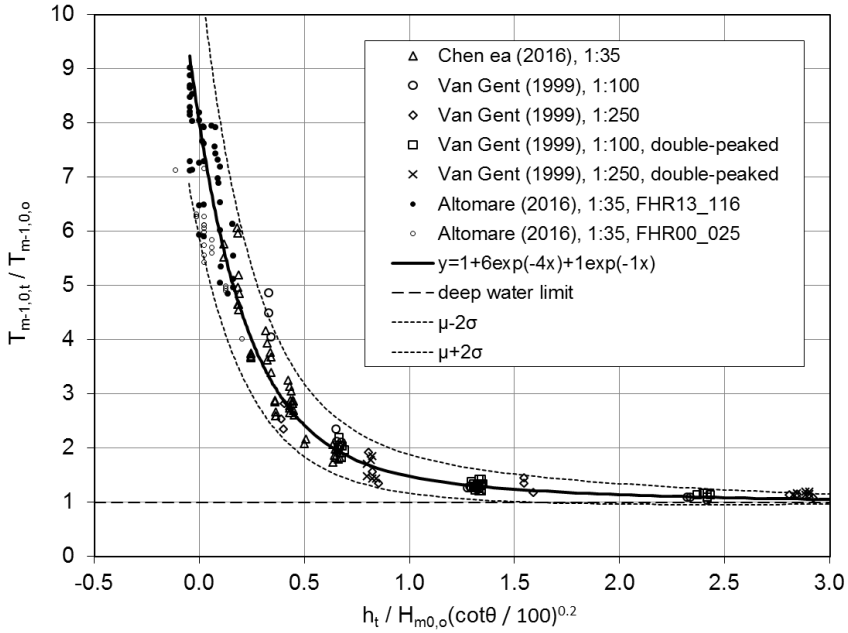

Figure 5. Data of the (increase in) measured wave period $T_{m-1,0}$ of long-crested waves on a straight mildly sloping foreshore, as a function of relative depth with slope correction. The solid line is the fit through the data given in eq. (4). The dashed lines indicate the +/-2σ (root-mean-square variation) error bands.

In Figure 5 all measurement data obtained with a straight foreshore are presented. The data collapse rather well. It can be seen that for shallow foreshores, the wave period $T_{m-1,0,t}$ increases slightly with decreasing depth, up to values of about 1.5 the offshore value. For very shallow foreshores $T_{m-1,0,t}$ increases quicker with depth, up to values of about 3.5 times the offshore value. For extremely shallow foreshores the increase in wave period is even more, up to values of about 8 times the offshore value at the water line (start of the swash zone).

The fit that is presented in Figure 5 for the increase of the spectral wave period in the test data is given by:

$$\frac{T_{\mathrm{m-1,0,t}}}{T_{\mathrm{m-1,0,o}}} - 1 = 6\exp\left(-4\,\tilde{h}\right) + \exp\left(-\tilde{h}\right), \qquad (4)$$

Two exponential terms are required to fit the data well both for the shallow and the extremely shallow foreshores. It can be seen that for extremely shallow conditions, the first term at the right hand side is dominant, and for shallow conditions the second term. When the equation is used for shallow foreshores ($\tilde{h} > 1$), only the second term on the right-hand side of eq. (4) can be used. The root-mean-square variation (σ) of the measurements compared to the fit (μ) varies linearly from σ/μ 0.18 at $\tilde{h} = 0$, to $\sigma/\mu = 0$ at $\tilde{h} = 4$. In Figure 5, the +/-2σ lines are

drawn. Eq. (4) gives slightly higher values than the best least-squares fit for all measurements. However, the numerical computations gave slightly larger values for $T_{m-1,0,t}$. In Figure 6, the 1D XBeach results are shown. It can be seen that the XBeach computation results follow the line of eq. (4) as well. From the data collapse of the different sources, it seems that the spectral wave period can be predicted fairly well for long-crested waves using the normalizations that were used. The water level at the toe that is reported, is the still water level before the tests, so without wave set-up. Therefore, negative water levels are given in Figure 5.

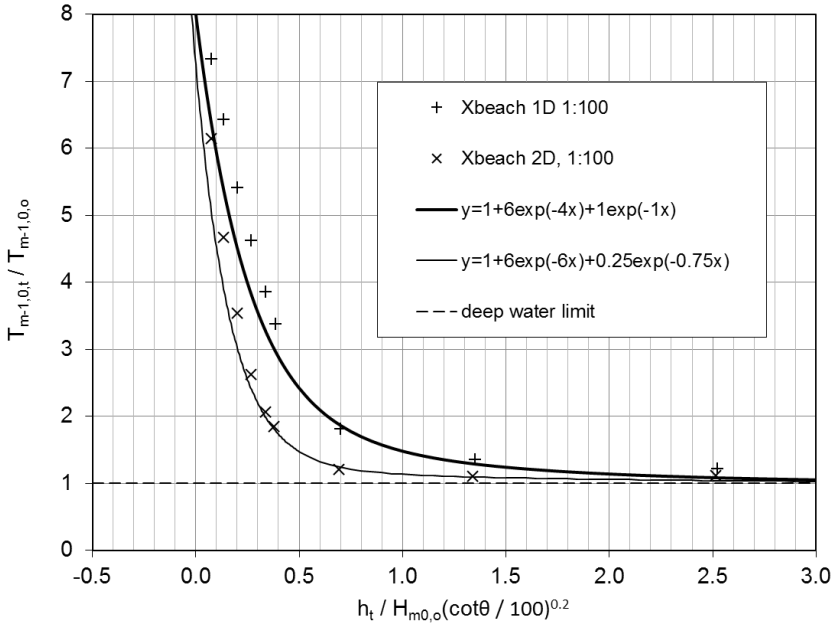

Figure 6. Numerical calculations of evolution of wave period $T_{m-1,0,t}$ as function of relative water depth for long-crested (XBeach 1D) and short-crested (XBeach 2D) waves.

4.1 Influence of directional spreading

All measurement data discussed until now were obtained from flume tests, i.e. long-crested wave conditions. However, for short-crested seas the generation mechanisms of the low-frequency wave energy may be different (see Section 2.3). Therefore additional 2D computations have been performed with XBeach. A snapshot of a 2D XBeach calculation with short-crested waves is given in Figure 7. The computational XBeach results with short-crested waves have been included in Figure 6. It can be seen that the increase of $T_{m-1,0,t}$ is less than that for the short-crested waves, and occurs much closers to shore than that for the long-created waves. The equation for the fit given in Figure 6 for the short-crested waves has a similar shape as eq. (4) and is given by:

$$\frac{T_{\mathrm{m-1,0,t}}}{T_{\mathrm{m-1,0,o}}} - 1 = 6\exp\left(-6\tilde{h}\right) + 0.25\exp\left(-0.75\tilde{h}\right) \ , \qquad (5)$$

403

404 Some existing data of a commercial project at Deltares (2011) is given in Figure 8 (squares
405 and circles). Otherwise identical tests were done with short- and long-crested waves on a
406 shallow foreshore. The results are plotted together with the fits of eqs. (4) and (5). For these
407 few measurements on a shallow foreshore, the wave period $T_{\mathrm{m-1,0,t}}$ agrees rather well with eqs.
408 (4) and (5).

409

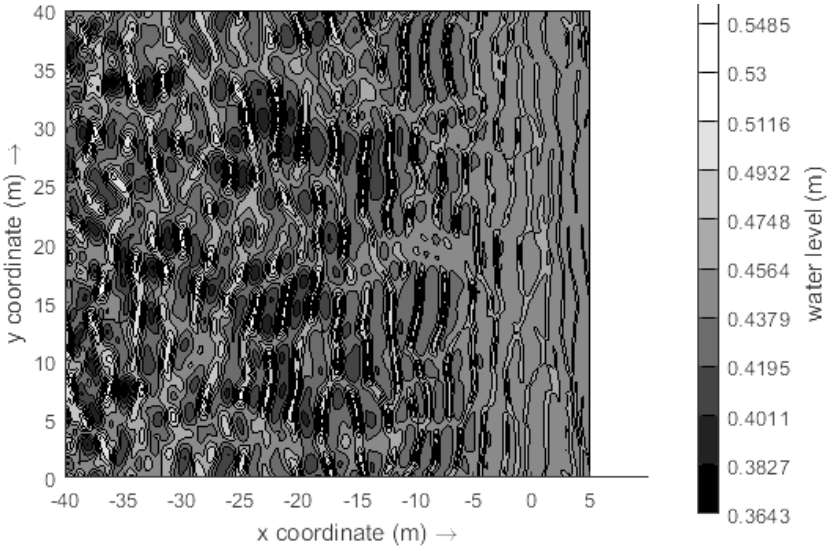

410

411 Figure 7. Snapshot of short-crested wave field over a shallow foreshore computed by XBeach (model scale).

412

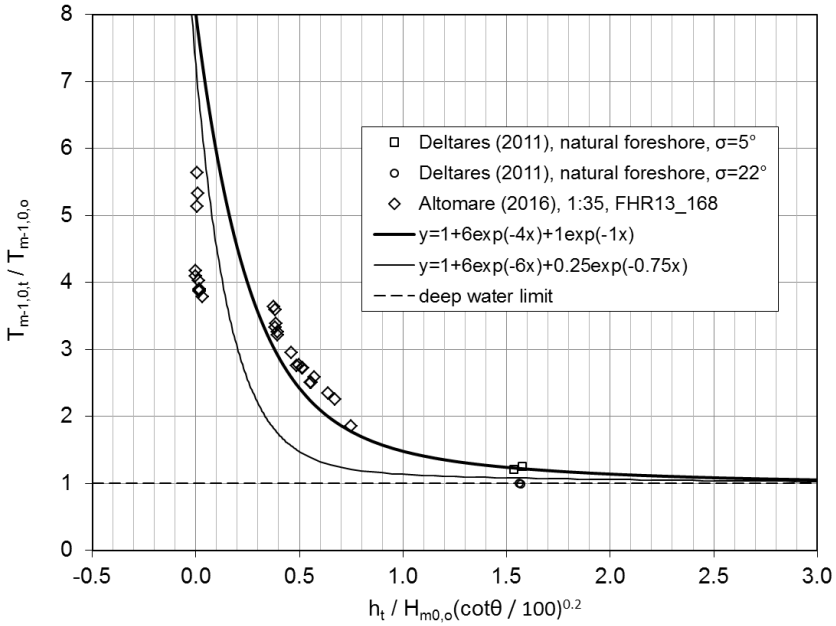

413

414 Figure 8. Evolution of wave period $T_{\mathrm{m-1,0}}$ as function of relative water depth compared to non-straight foreshores.

4.2 Influence of non-straight foreshore

Some scarce data was obtained with non-straight foreshores. This data is compared to the fits for the straight foreshore in Figure 8.

The data of Deltares (2011) that is presented in Figure 8 was obtained for an irregular natural foreshore. The few measurements represent shallow water conditions. Despite the irregular nature of the foreshore, the resulting wave period, which has a limited influence of this shallowness, is still comparable to the formula.

In the foreshore of test series FHR 13_168 (Altomare et. al. (2015) a change in foreshore slope was situated at depths of 7 to 10 times the offshore wave height. The results for the very shallow foreshore conditions are close to the general trend of eq. (4). However, the results for the extremely shallow foreshore conditions are much lower than eq. (4). It is not clear whether this change in foreshore slope (at a rather deep level) or another influence has altered the wave period evolution for these tests with the lower water levels. This aspect is further discussed in the next section.

5. Discussion

First we discuss whether the application linear wave generation influences the results. The tests of Chen et al. (2016) and most of Altomare et al. (2016; FHR13_116, FHR00_025) were made using linear wave generation. Using this kind of wave generation might increase the value of $T_{m\text{-}1,0,t}$, as spurious low-frequency waves are created. However, the tests with linear wave generation do not seem to have a different trend than those with 2nd order wave generation. Only the results from dataset 13_168 with 2nd order wave generation (Altomare et al., 2016), show much lower values of $T_{m\text{-}1,0,t}$ / $T_{m\text{-}1,0,o}$ for extremely shallow water at the toe, see Figure 8, while the results did align for the very shallow foreshore cases. However, in these tests also the foreshore was not straight. In the XBeach computations, which do have 2nd order wave generation, the wave periods increase to even somewhat larger values than were measured for extremely shallow foreshore depths. So from these results it seems that the 1st order wave generation does not have a large influence.

For more complicated cross sections, such as bar systems, eq. (5) has not yet been validated by the few data point presented in Section 4. However, as the bed slope has a relatively small influence in the parameter defined in eq. (3), it could be expected that the main trend might hold for somewhat more complex geometries. The few data points that were given in Section 4.2 do seem to corroborate this. De Bakker et al. (2016) also observed that the influence of a concave or convex foreshore on the low-frequency wave energy evolution was much less than

that of the (average) slope. Furthermore, for oblique wave attack, refraction will influence the waves.

The degree of mildness of a foreshore slope can be estimated using a steepness parameter like β_b in eq. (2). As eq. (2) was developed for regular bound waves (bichromatic primary waves), it is assumed that the mean breaker depth h_b is equal to $2H_{m0,o}$, and that the angular frequency of the bound long waves is $\omega = 2\pi/5T_{m-1,0,o}$. Using these assumptions, a rough estimate of the steepness parameter β_b for the present tests was 0.02 to 0.35, with values lower than 0.3 for more than 90% of the tests. In Section 2.3, it was discussed that for $\beta_b < 0.3$ the mild-slope type of long-wave generation according to Longuet-Higgins and Stewart (1962) occurs. Hence, we can conclude that the present equation is valid for mild slopes. It is not known whether the development of the mean wave energy period $T_{m-1,0}$ will be the same for steeper slopes than presently studied (1:35). In terms of a newly defined slope parameter, the limiting slope for the present equation is obtained by rewriting $\beta_b < 0.35$ including the previously mentioned assumptions for long wave period and breaker depth, which yields as range of validity:

$$\theta\, T_{m-1,0,o}\sqrt{\frac{g}{H_{m0,o}}} < 0.62\ . \qquad (6)$$

Most tests were done with JONSWAP spectra that are characterized by a relatively narrow peak. Other spectral shapes than JONSWAP were only included for $h_t / H_{m0,o} > 0.67$ (Van Gent, 1999a), but for this region there was a good data collapse. Hence, it seems that the wave period $T_{m-1,0,t}$ is not very dependent on the offshore spectrum type. These different spectral shapes were double-peaked spectra, that considered of two superimposed JONSWAP spectra with the same peakedness. So, strictly speaking, the comparable results for the single-peaked and double-peaked spectra might be due to the fact that each peak leads to the same type of low-frequency wave generation without much interaction between the peaks. Hence, spectra with separate broader peaks may still yield somewhat different wave periods $T_{m-1,0,t}$.

6. Conclusions

The spectral mean wave energy period $T_{m-1,0}$ has become accepted as a characteristic period when describing the hydraulic attack on coastal structures. A prediction formula has been derived for the wave period $T_{m-1,0}$ on shallow to extremely shallow foreshores with a mild slope. A shallow foreshore is defined here as a bathymetry seaward of a structure that is deeper than $h_t/H_{m0,o} = 4$, a very shallow foreshore as $h_t/H_{m0,o} < 1$, and an extremely shallow

foreshore as $h_t/H_{m0,o} < 0.3$. A mild slope of the foreshore is defined here as $\theta\, T_{m-1,0,o}\sqrt{g/H_{m0,o}} < 0.62$ (see Figure 1 for the nomenclature). The prediction formula for $T_{m-1,0}$ was determined based on tests and calculations for straight linear foreshore bed slopes and perpendicular wave attack. The wave period $T_{m-1,0}$ increases drastically when the water depth decreases, up to about 8 times the offshore value for extremely shallow foreshores. This increase of $T_{m-1,0}$ with decreasing depth was somewhat less for milder slopes. For short-crested wave fields the strong increase of the wave period $T_{m-1,0}$ starts closer to shore (at smaller water depths) than for long-crested wave fields. For some cases with double-peaked offshore spectra and irregular foreshores the increase of the wave period $T_{m-1,0}$ with decreasing depth follows the same trend as for long-crested waves. However, it is recommended to determine and/or extend the range of validity of the formulations for different degrees of short-crestedness, spectral peak width, average foreshore slope, and foreshore slope irregularities. A good prediction of the wave period $T_{m-1,0,t}$ will improve the capability to make (conceptual) designs for coastal structures on shallow to extremely shallow foreshores.

Acknowledgements

We thank the anonymous reviewers for their constructive comments, and dr. Marion Tissier and dr. James Salmon for proof-reading the manuscript. The data of Chen et al. (2016) that are used in this paper were obtained in research project Hydraulic impact of overtopping waves on a multi-functional dike, project number 12176 (1.1.1), funded by technology foundation STW.

List of symbols

f	: frequency	[s^{-1}]
g	: gravitational acceleration	[ms^{-2}]
h	: water depth	[m]
h_b	: a mean breaking depth	[m]
H_{m0}	: spectral significant wave height, = $4\sqrt{m_0}$	[m]
k_p	: wave number based on the peak period, $=2\pi/(gT^2_p/2\pi)$	[m^{-1}]
L_o	: fictitious offshore wave length,= $g/2\pi\ T^2_{m-1,0,o}$	[m]
m_n	: n^{th} order moment of surface elevation	[m^2/s^n]
P	: wave energy flux	[Wm^{-1}]
$s_{m-1,0,o}$	: offshore wave steepness, = $H_{m0,o}$ / $\frac{g}{2\pi}T_{m-1,0,o}{}^2$	[-]
S	: the spectral density of the water surface elevation	[m^2s]
t	: time	[s]
$T_{1/3}$	: significant wave period, mean period of the highest third of the waves in a record	[s]
T_m	: mean wave period	[s]
$T_{m-1,0}$	: spectral mean wave energy period, = m_{-1}/m_0	[s]
T_p	: peak wave period	[s]
β_b	: kind of surf-similarity parameter for bound long waves	[-]
η	: the surface elevation	[m]
θ	: foreshore slope	[rad]
μ	: mean value	
σ	: standard deviation	
ω	: angular frequency (of bound long waves)	[s^{-1}]
$_o$	: subscript indicating an offshore location	
$_t$	: subscript indicating a location at the toe of a structure	

References

Altomare, C., T. Suzuki, X. Chen, T. Verwaest, A. Kortenhaus. (2016) *Wave overtopping of sea dikes with very shallow foreshores.* Coastal Engineering, Volume 116, October 2016, pp. 236-257, ISSN 0378-3839.

Battjes, J.A. (1969) *Discussion of paper by J.N. Svašek: Statistical evaluation of wave conditions in a deltaic area.* Proc. Symp. on Research on Wave Action. Vol. 1, paper 1. Waterloopkundig Laboratorium (presently Deltares), Delft, the Netherlands.

Battjes, J.A. and Groenendijk, H.W. (2000). *Wave height distributions on shallow foreshores*. Coastal Engineering 40(3), pp 161–182.

Battjes, J.A., H.J. Bakkenes, T.T. Janssen, and A.R. van Dongeren (2004) *Shoaling of subharmonic gravity waves*. Journal of Geophysical Research 109, C02009, doi:10.1029/2003JC001863.

Chen, X., B. Hofland, W.S.J. Uijttewaal. (2016) *Maximum overtopping forces on a dike-mounted wall with a shallow foreshore.* Coastal Engineering 116, October 2016, pp. 89–102.

CIRIA, CUR, CETMEF. (2007) *The Rock Manual. The use of rock in hydraulic engineering (2nd edition).* C683, CIRIA, London

De Bakker, A. T. M., M. F. S. Tissier, and B. G. Ruessink (2016) *Beach steepness effects on nonlinear infragravity-wave interactions: A numerical study*. J. Geophys. Res. Oceans, 121, 554–570, doi:10.1002/2015JC011268.

Dekker, J., S. Caires,.M.R.A. van Gent (2007) *Reflection of non-standard wave spectra by sloping structures.* Proc. Coastal Structures 2007.

Deltares (2011). Technical report no. 1204569-000-HYE-0012. Deltares, October 2011.

EurOtop (2016) Manual on wave overtopping of sea defences and related structures. An overtopping manual largely based on European research, but for worldwide application. Authors: Van der Meer, J.W. (ed.), Allsop, N.W.H., Bruce, T., De Rouck, J., Kortenhaus, A., Pullen, T., Schüttrumpf, H., Troch, P. and Zanuttigh, B. Pre-release of 2nd edition, October 2016 www.overtopping-manual.com.

Goda, Y. (1975) Irregular wave deformation in the surf zone. Coastal Engineering in Japan 18, 13–26 (JSCE)

Goda, Y. (2009) *Derivation of unified wave overtopping formulas for seawalls with smooth, impermeable surfaces based on selected CLASH datasets.* Coastal Engineering 56(4), pp. 385–399.

Herbers, T. H. C., S. Elgar, and R. T. Guza (1994) *Infragravity-frequency (0.005-0.05 Hz) motions on the shelf. Part I: Forced waves.* J. Phys. Oceanogr., 24, 917–927.

Holterman, S. R. (1998) *Wave runup on dikes with a shallow foreshore. (In Dutch) Golfoploop op dijken met ondiep voorland.* MSc thesis, TU Delft, Delft. http://repository.tudelft.nl

Longuet-Higgins, M. S., and R. W. Stewart (1962) *Radiation stress and mass transport in gravity waves, with application to 'surf beats'*. J. Fluid Mech., 13, 481–504.

Mansard and Funke (1980). *The measurement of incident and reflected spectra using a least squares method*. Proceedings 17th International Coastal Engineering Conference, ICCE, pp. 154–172.

Munk, W. H. (1949), Surf beats, Eos Trans AGU, 30, 849– 854.

Pozueta, B., M.R.A. van Gent, H. Van den Boogaard, J.R. Medina (2005) *Neural network modelling of wave overtopping at coastal structures.* Coastal Engineering 2004: proc. 29th int. conference Lisbon, Portugal, 19-24 September 2004, Vol.4 ; p. 4275-4287

Roelvink, D., A. Reniers, A. van Dongeren, J. Van Thiel de Vries, R. McCall, J. Lescinski (2009) *Modeling storm impacts on beaches, dunes and barrier islands.* Coastal Engineering 56, 1133–1152.

Smit, P., Stelling, G., Roelvink, J., Van Thiel de Vries, J., McCall, R., Van Dongeren, A., ... & Jacobs, R. (2010). *XBeach: Nonhydrostatic model: Validation, verification and model description.* Tech. rept. Delft University of Technology, Delft, the Netherlands.

Stelling, G. and M. Zijlema (2003). *An accurate and efficient finite-difference algorithm for non-hydrostatic free-surface flow with application to wave propagation.* International Journal for Numerical Methods in Fluids 43(1): 1-23.

Suzuki, T., C. Altomare, T. Verwaest, K. Trouw and M. Zijlema (2014) *Two-dimensional wave overtopping calculation over a dike in shallow foreshore by SWASH*. Proceedings ICCE 2014.

Symonds, G., D. A. Huntley, and A. J. Bowen (1982) *Two dimensional surfbeat: Long wave generation by a time varying breakpoint*. J. Geophys. Res., 87, 492– 498.

TAW (2002) *Technical Report Wave Run-up and Wave Overtopping at Dikes*. Delft, the Netherlands. Report of the Technische Adviescommissie voor de Waterkeringen.

Tucker, M. J. (1950), *Surf beats: Sea waves of 1 to 5 min. period*. Proc. R. Soc. London, Ser. A, 202, 565– 573.

U.S. Army Corps of Engineers (2002) *Coastal Engineering Manual (CEM)*. Engineer Manual 1110-2-1100, U.S. Army Corps of Engineers, Washington, D.C. (6 volumes).

Van Dongeren, A., J. Battjes, T. Janssen, J. van Noorloos, K. Steenhauer, G. Steenbergen, and A. Reniers (2007) *Shoaling and shoreline dissipation of low-frequency waves.* Journal of Geophysical Research, Vol. 112.

Van Gent, M.R.A. (1999a) *Physical model investigations on coastal structures with shallow foreshores*. Delft Hydraulics (Deltares) Report H3608, January 1999, Delft.

Van Gent, M.R.A. (1999b), *Wave run-up and wave overtopping for double peaked wave energy spectra*. Delft Hydraulics (Deltares) Report H3351-2, January 1999, Delft.

607 Van Gent, M.R.A. (2001), *Wave run-up on dikes with shallow foreshores*. ASCE, Journal of
608 Waterway, Port, Coast. & Ocean Engineering., Vol.127, No. 5.

609 Van Gent, M.R.A., Smale, A.J. and Kuiper, C. (2004). *Stability of rock slopes with shallow foreshores.*
610 In: J.A. Melby (ed), Proc 4th int coastal structures conf, Portland, OR, 26–30 Aug 2003.
611 ASCE, Reston, VA.

612 Zanuttigh, B., and J.W. van der Meer (2008) *Wave reflection from coastal structures in design*
613 *conditions.* Coastal Engineering Volume 55, Issue 10, October 2008, Pages 771-779

614 Zijlema, M., Stelling, G.S. and Smit P. (2011) SWASH: An operational public domain code for
615 simulating wave fields and rapidly varied flows in coastal waters. Coastal Engineering 58.
616 pp. 992-1012.